

# Analyst

Accepted Manuscript



This is an *Accepted Manuscript*, which has been through the Royal Society of Chemistry peer review process and has been accepted for publication.

*Accepted Manuscripts* are published online shortly after acceptance, before technical editing, formatting and proof reading. Using this free service, authors can make their results available to the community, in citable form, before we publish the edited article. We will replace this *Accepted Manuscript* with the edited and formatted *Advance Article* as soon as it is available.

You can find more information about *Accepted Manuscripts* in the [Information for Authors](#).

Please note that technical editing may introduce minor changes to the text and/or graphics, which may alter content. The journal's standard [Terms & Conditions](#) and the [Ethical guidelines](#) still apply. In no event shall the Royal Society of Chemistry be held responsible for any errors or omissions in this *Accepted Manuscript* or any consequences arising from the use of any information it contains.

1  
2  
3  
4  
5  
6  
7  
8  
9  
10  
11  
12  
13  
14  
15  
16  
17  
18  
19  
20  
21  
22  
23  
24  
25  
26  
27  
28  
29  
30  
31  
32  
33  
34  
35  
36  
37  
38  
39  
40  
41  
42  
43  
44  
45  
46  
47  
48  
49  
50  
51  
52  
53  
54  
55  
56  
57  
58  
59  
60

1       **Fabrication of Novel Chemosensors Composed of Rhodamine Derivative for**  
2       **Detection of Ferric Ion and Mechanism Studies on the Interaction between**  
3                               **Sensor and Ferric Ion**

5       Dongjian Shi<sup>a</sup>, Ming Ni<sup>a</sup>, Jing Luo<sup>a</sup>, Mitsuru Akashi<sup>b</sup>, Xiaoya Liu<sup>a</sup>, Mingqing Chen<sup>a\*</sup>

7       <sup>a</sup> The Key Laboratory of Food Colloids and Biotechnology Ministry of Education,  
8       School of Chemical and Material Engineering, Jiangnan University, Wuxi 214122, P.  
9       R. China

10      <sup>b</sup> Department of Applied Chemistry, Graduate School of Engineering, Osaka  
11      University, 2-1 Yamadaoka, Suita 565-0871, Japan

14      Corresponding Author  
15      Prof. Mingqing Chen  
16      E-mail: [mqchen@jiangnan.edu.cn](mailto:mqchen@jiangnan.edu.cn)  
17      TEL: 86-518591019, FAX: 86-51085917763

18

Analyst Accepted Manuscript

## Abstract

Although many rhodamine based fluorescence sensors were reported to detect metal ions with high sensitivity and selectivity, there are very few reports to study the mechanisms of detection and the interaction between probe and metal ions. This paper presents to detect ferric ions by novel fluorescence chemosensors and study the mechanism in detail. A novel probe AD-MAH-RhB was designed and synthesized from rhodamine B (RhB), adamantyl (AD), ethylene diamine and maleic anhydride (MAH). AD-MAH-RhB could detect  $\text{Fe}^{3+}$  in aqueous solution. The mechanism was explored by HSAB principle and FTIR and mass spectra. The results suggested that  $\text{Fe}^{3+}$  bound with amine and oxygen atoms in AD-MAH-RhB to form a complex composed of 2:1 stoichiometry of  $\text{Fe}^{3+}$  and the probe. Moreover, computational simulations were employed to further investigate the detection mechanism. The calculated results showed that  $\text{Fe}^{3+}$  could conjugate with AD-MAH-RhB probe to form stable complex, which induced by synergetic effects of the suitable space and distance of Van der Waals. However,  $\text{Hg}^{2+}$  was found to disturb this detection and formed a complex with 1:2 stoichiometry of  $\text{Hg}^{2+}$  and AD-MAH-RhB. Then, another probe,  $\beta$ -cyclodextrin modified polymaleicanhydride (PMAH-CD) inclusive AD-MAH-RhB (PMAH-CD/AD-MAH-RhB) was fabricated by inclusion interaction between CD and AD. PMAH-CD@AD-MAH-RhB showed high selectivity and sensitivity to  $\text{Fe}^{3+}$  in aqueous solution by eliminating the interruption of  $\text{Hg}^{2+}$ , possibly due to the high hydrogen interaction among the probes to inhibit the form stable complex with  $\text{Hg}^{2+}$ .

1  
2  
3  
4  
5  
6  
7  
8  
9  
10  
11  
12  
13  
14  
15  
16  
17  
18  
19  
20  
21  
22  
23  
24  
25  
26  
27  
28  
29  
30  
31  
32  
33  
34  
35  
36  
37  
38  
39  
40  
41  
42  
43  
44  
45  
46  
47  
48  
49  
50  
51  
52  
53  
54  
55  
56  
57  
58  
59  
60

41     **Keywords:** fluorescence sensor, Rhodamine derivative, detection, mechanism study

42

## 1. Introduction

Metal ions such as  $\text{Fe}^{3+}$ ,  $\text{Hg}^{2+}$ ,  $\text{Cr}^{3+}$ , from industrial effluents become significant pollution for the environment. Since these pollutants can be easily absorbed by aquatic organisms, bioaccumulated and spread along the food chain, the analysis and detection of the metal ions in water are important subjects for biology and environmental chemistry<sup>[1]</sup>. Consequently, over the last few decades, considerable efforts have been devoted to developing fluorescent chemosensors for metal ions with high selectivity, sensitivity and reliability<sup>[2-9]</sup>. Some fluorescent chemosensors that composed of chromophores such as fluorescein<sup>[10-11]</sup>, rhodamine<sup>[12]</sup>, coumarin<sup>[13]</sup> and recognition groups such as crown ether<sup>[14]</sup>, calixarene<sup>[15]</sup>, polyamine<sup>[16]</sup>, have been prepared for detection of metal ions.

Rhodamine scaffold is an ideal template chromophore for the construction of chemosensors because they have large molar extinction coefficient, long excitation and emission wavelengths and high fluorescence quantum yields<sup>[17-18]</sup>. Moreover, rhodamine derivatives with a spirolactam structure are colorless and nonfluorescent, whereas a ring-opened amide form of rhodamine derivative gives rise to both chromogenic and fluorogenic response to facilitate an OFF/ON-type fluorescent detection. Therefore, a number of fluorescence sensors have been developed based on rhodamine derivatives with different recognition groups for detection of metal ions. Li group<sup>[19]</sup> reported a fluorophore dye containing rhodamine and a naphthalimide moiety to be as a  $\text{Cr}^{3+}$ -selective fluorescent probe. Hu et al.<sup>[20]</sup> reported a colorimetric and fluorescent chemosensor based on a rhodamine 6G phenylurea conjugate could

65 recognize Fe(III) ions. Yook and Tae groups<sup>[21-22]</sup> prepared a series of  
66 rhodamine-based fluorescent and colorimetric sensors for the detection of Hg and Pt  
67 ions. These reported probes showed highly selective and sensitive to special metal  
68 ions. However, the recognition mechanism was seldom studied in these examples.  
69 Thus, some existing problems should be explained and solved, such as why the  
70 recognition groups showed the selectivity towards different metal ions although they  
71 containing similar cooperative atoms or groups, what is the interaction between  
72 sensors and metal ions, how to construct a fluorescence sensor to detect a designated  
73 metal ion, and which principle should be followed during the structure design of the  
74 sensor.

75 Since the structure of a probe-metal ion complex is complicated and the binding  
76 interaction between probe and metal is concerned several aspects such as metal size,  
77 outer shell electrons of metal, Van der Waals force, and so on, it is difficult to explain  
78 the recognition mechanism very well by experiment method. Compared with  
79 experimental methods, computational simulations are time-saving and eco-friendly<sup>[23]</sup>.  
80 They have been employed to design a desired structure with excellent performance in  
81 quantum-chemical (QC) area. However, there are few researches to calculate the  
82 structure of rhodamine based fluorescent chemosensor and investigate the relationship  
83 between probe and metal ion by computational simulations.

84 Ferric ions are very important to our body, and will cause anemia and breathing  
85 problems if deficient, while will be toxic to body when they are at levels exceeding  
86 the capacity of safe consumption<sup>[24]</sup>. Thus, our aim is to detect ferric ions in aqueous

1  
2  
3  
4 87 solution by a designed rhodamine derivative with high sensitivity and selectivity. In  
5  
6 88 order to design a probe for recognition of ferric ions, we should firstly know the  
7  
8 89 chemical properties of the recognition groups and metal ions. Metal ions can be  
9  
10 90 divided into two parts: hard acid and soft acid, and the recognition groups were also  
11  
12 91 divided into hard base and soft base. According to HSAB principle that “hard likes  
13  
14 92 hard and soft likes soft”, which was reported by Pearson<sup>[25]</sup>, Fe(III) ion is a hard acid  
15  
16 93 and can form a stable complex with the hard bases such as carbonyl and amide groups.  
17  
18 94 Thus, in this work, ethylene diamine and maleic anhydride (MAH) were selected as  
19  
20 95 receptors to recognize Fe(III) ion, and rhodamine B (RhB) was as a fluorophore.  
21  
22 96 Adamantyl (AD) was also introduced into the probe for further modification of the  
23  
24 97 probe structure with cyclodextrin via host-guest interaction. Then, the novel  
25  
26 98 fluorescent probe (AD-MAH-RhB) was developed based on RhB, ethylene diamine,  
27  
28 99 MAH and AD, as Scheme 1a. The sensitivity and selectivity of the probes to Fe ions  
29  
30 100 were detected. The relatively recognition mechanisms were investigated in detail by  
31  
32 101 HSAB Principle, FTIR and mass spectra. Moreover, computational simulation was  
33  
34 102 employed to investigate the relationship between the structure and the selectivity of  
35  
36 103 the probe, and to determine what the key factors are that will improve the selectivity  
37  
38 104 of the probe. Furthermore, for improvement of the selectivity to Fe<sup>3+</sup>, another probe  
39  
40 105 with complicated structure (Scheme 1b) was designed and prepared by  
41  
42 106 AD-MAH-RhB and cyclodextrin functionalized polymaleicanhydride (PMAH-CD) via  
43  
44 107 host-guest interaction. The high selectivity of the probe to Fe ion was detected. These  
45  
46 108 probes could be used as sensor to the great potential application for detection. The  
47  
48  
49  
50  
51  
52  
53  
54  
55  
56  
57  
58  
59  
60

1  
2  
3  
4 109 mechanism study might help to design a fluorescence sensor effectively for detection  
5  
6 110 of a desired metal ion.  
7

## 8 9 111 **2. Experimental Section**

### 10 11 112 **2.1 Materials and instruments**

12  
13 113 Tosyl chloride (TsCl), 1-aminoadamantane (AD-NH<sub>2</sub>), ethylene diamine (EDA),  
14  
15  
16 114 and maleic anhydride (MAH) were bought from Sigma-Aldrich Chem. Co., and used  
17  
18 115 without further purification.  $\beta$ -Cyclodextrin (CD) was purchased from Sigma-Aldrich  
19  
20 116 Chem. Co., and purified by recrystallization. All metallic salts, such as Ba(NO<sub>3</sub>)<sub>2</sub>,  
21  
22  
23 117 CdCl<sub>2</sub>·2.5H<sub>2</sub>O, Co(NO<sub>3</sub>)<sub>2</sub>·6H<sub>2</sub>O, FeCl<sub>3</sub>·6H<sub>2</sub>O, MgCl<sub>2</sub>, KCl, Ni(NO<sub>3</sub>)<sub>2</sub>·6H<sub>2</sub>O, AgNO<sub>3</sub>,  
24  
25  
26 118 CuCl<sub>2</sub>, and Hg(NO<sub>3</sub>)<sub>2</sub>, were purchased from Sinopharm Chemical Reagent Co. Ltd,  
27  
28 119 and theirs aqueous solutions were prepared with ultrapure water from a Millipore  
29  
30 120 autopure WR600A system (Millipore, Ltd. USA).  
31

32  
33 121 UV-vis spectrum was recorded on a TU-1901 spectrophotometer (Beijing Purkinje  
34  
35 122 General Instrument Co. Ltd). Fourier transform infrared spectroscopy (FTIR)  
36  
37 123 spectrum (Nicolet iN10) was recorded on an attenuated total reflection (ATR) method  
38  
39 124 with a FT-IR spectrometer. Fluorescence emission spectrum was recorded with a  
40  
41  
42 125 varianinc Cary Eclipse spectrophotometer at an excitation wavelength of 541nm. All  
43  
44 126 the spectroscopic measurements were performed at least in triplicate and averaged.  
45  
46  
47 127 All the computational simulations were performed with GAUSSIAN03<sup>[26]</sup>.  
48

### 49 50 51 128 **2.2 Synthesis of AD-MAH-RhB probe**

52  
53  
54 129 Rhodamine B was synthesized in a similar manner to reported methods<sup>[25]</sup>. Then,  
55  
56 130 MAH (1 mmol), RhB (1 mmol) and 4-dimethylamiopyridine (DMAP, 0.15 mmol)  
57  
58  
59  
60



1  
2  
3  
4 131 were dissolved in DMSO. 1-Ethyl-3-(3-Dimethylaminopropyl) carbodiimide (EDC, 1  
5  
6 132 mmol) and hydroxybenzotriazole (HOBt, 1 mmol) were added into the above solution.  
7  
8  
9 133 By activated for 1 h, 1-aminoadamantane (AD-NH<sub>2</sub>, 1 mmol) was added and started  
10  
11 134 reaction at room temperature (Scheme S1). After predetermined time, red powder was  
12  
13  
14 135 obtained by removing solvent under reduced pressure and purified by silica gel  
15  
16 136 column chromatography in CH<sub>2</sub>Cl<sub>2</sub> to give purified AD-MAH-RhB (367 mg, 53 %).  
17  
18  
19 137 <sup>1</sup>H NMR (400MHz, CDCl<sub>3</sub>, ppm, Figure S1): 7.88-7.85 (1H), 7.45-7.42 (2H),  
20  
21 138 7.09-7.07 (1H), 6.44-6.26 (8H), 3.37-3.26 (12H), 1.90-1.70 (15H, adamantyl imine),  
22  
23  
24 139 1.18-1.14 (12H). ESI m/z[M+Na<sup>+</sup>] : 738.5.

### 240 **2.3 Synthesis of cyclodextrin functionalized polymaleicanhydride (PMAH-CD)**

25  
26  
27  
28  
29 141 Polymaleicanhydride (PMAH) was synthesized by Reversible Addition  
30  
31 142 Fragmentation Chain Transfer Polymerization (RAFT) using a chain transfer agent  
32  
33  
34 143 which prepared in a reported method<sup>[27]</sup>. As shown in Scheme S2, MAH (5 g),  
35  
36 144 S,S'-bis(α,α'-dimethyl-α'-acetic acid)-trithiocarbonate (143 mg) and AIBN (84 mg)  
37  
38  
39 145 were dissolved in toluene at 0 °C under N<sub>2</sub> atmosphere. PMHA was obtained by  
40  
41 146 dialyzed and dried after reacted at 80 °C for 8 h, and the yield was about 30 % (1.5 g).  
42  
43  
44 147 The molecular weight of PMAH was 3710, which was measured by GPC.

45  
46  
47 148 Ethylene diamine mono-substituted β-cyclodextrin (EDA-β-CD) was synthesized  
48  
49 149 according to the reported methods<sup>[28]</sup>. Then, PMAH (0.0376 g), DMAP (20 mg),  
50  
51 150 HOBt (137 mg), EDC (191 mg) and EDA-β-CD (12 mg) were dissolved in 10 ml of  
52  
53  
54 151 DMF (Scheme S2). After reacted for 12 h, 40 mg of product PMAH-CD was dialyzed  
55  
56  
57 152 and dried. The yield was 80 %. <sup>1</sup>H NMR (400MHz, D<sub>2</sub>O, ppm, Figure S2): 5.0-5.19

(7H), 3.26-3.91 (42H), 1.13-1.15 (12H).

### 2.3 Preparation of the supramolecular complex PMAH-CD/AD-MAH-RhB

PMAH-CD ( $5.5 \times 10^{-6}$  mol) was dissolved in 40 mL of deionized water. Then, the same concentration of AD-MAH-RhB in 10 mL of ethanol was added slowly into the PMAH-CD aqueous solution. The mixed solution was stirred for 2 d at room temperature. The inclusion complex was obtained by dialysis and drying under reduced pressure <sup>[29]</sup>.

### 2.4 Detection procedure

Standard solution of  $\text{Fe}^{3+}$  ( $7 \times 10^{-3}$  mol  $\text{L}^{-1}$ ) was obtained by dissolving 189.2 mg  $\text{FeCl}_3 \cdot 6\text{H}_2\text{O}$  solid in ultrapure water. The binding complex solutions of AD-MAH-RhB and  $\text{Fe}^{3+}$  were obtained by mixing 5 mL of the stocked AD-MAH-RhB solution and 0.2, 0.5, 0.7, 1.0, 1.5, 2.0, 2.5 mL of  $\text{Fe}^{3+}$  standard solution in a 25 mL volumetric flask, respectively. The PMAH-CD/AD-SRhB@Fe complex solutions were the same process as mentioned above. The concentrations of  $\text{Fe}^{3+}$  in the resultant solutions were 0, 1, 9, 10, 15, 23, 30 and 38 mg  $\text{L}^{-1}$ . The fluorescences of all the samples before and after formed complexes were measured by excitation at 514 nm. FTIR spectra of the AD-MAH-RhB solution and the complexes with  $\text{Hg}^{2+}$  and  $\text{Fe}^{3+}$  were carried out by ATR method. The complex for mass spectrum measurement was prepared by mixing AD-MAH-RhB and metal ions in methanol.

## 3. Results and Discussion

### 3.1 Sensitivity and selectivity of AD-MAH-RhB

Depending on HSAB principle,  $\text{Fe}^{3+}$  is a hard acid and likes hard base ligand. The

175 prepared AD-MAH-RhB contains the carbonyl and amine groups. Thus,  
176 AD-MAH-RhB could detect  $\text{Fe}^{3+}$ . The solution of AD-MAH-RhB was colorless and  
177 did not exhibit any absorption, which was coincident with the property of the  
178 spirocycle RhB derivatives by UV/vis spectrum. By adding  $\text{Fe}^{3+}$  ions to the  
179 AD-MAH-RhB solution, the color of the mixture changed to rose red immediately.  
180 UV-vis spectra confirmed that  $\text{Fe}^{3+}$  induced an increment in the absorption of  
181 AD-MAH-RhB at 564 nm, as shown in Figure 1a, indicating addition of  $\text{Fe}^{3+}$  can  
182 promote the formation of the open-ring state of the RhB moieties. The absorption  
183 intensity increased with increasing the  $\text{Fe}^{3+}$  concentration. Figure 1b shows the  
184 fluorescence changes in the probe-metal complex upon addition of  $\text{Fe}^{3+}$ . By excitation  
185 at 541 nm, there was almost no emission profile of RhB in the absence of  $\text{Fe}^{3+}$ . Upon  
186 addition of  $\text{Fe}^{3+}$ , a strong emission peak at around 587 nm appeared and increased  
187 gradually with increasing the concentration of  $\text{Fe}^{3+}$ . The detection limit was calculated  
188 to reach  $8.3 \text{ mg L}^{-1}$ . These results confirmed that the probe could detect  $\text{Fe}^{3+}$  in  
189 aqueous solution with low detection limit.

190 High selectivity is an important index to know whether the rhodamine probe is an  
191 excellent probe. Thus, fluorescent and absorption spectra of AD-MAH-RhB to other  
192 traditional metal ions were examined, such as  $\text{Hg}^{2+}$ ,  $\text{Cd}^{2+}$ ,  $\text{Cu}^{2+}$ ,  $\text{Ba}^{2+}$ ,  $\text{Ag}^{+}$ ,  $\text{Zn}^{2+}$ ,  $\text{Co}^{2+}$ ,  
193  $\text{K}^{+}$ ,  $\text{Mg}^{2+}$ ,  $\text{Ni}^{2+}$  and  $\text{Pb}^{2+}$ . Figure 2 shows the fluorescence intensity of the  
194 AD-MAH-RhB aqueous solution ( $1.4 \times 10^{-4} \text{ M}$ ) upon addition of different metal ions  
195 with the concentration of  $1 \times 10^{-2} \text{ M}$  in pH 7.0. From Figure 2, it clearly showed that  
196  $\text{Fe}^{3+}$  and  $\text{Hg}^{2+}$  induced a prominent fluorescence increment, whereas other metal ions

1  
2  
3  
4 197 did not show any obvious fluorescence enhancement at 587 nm of emission peak as  
5  
6 198 well as no color change. Depending on the HSAB principle,  $\text{Fe}^{3+}$ ,  $\text{Ba}^{2+}$  and  $\text{K}^{+}$  are  
7  
8  
9 199 hard acid, whereas  $\text{Hg}^{2+}$ ,  $\text{Cd}^{2+}$  and  $\text{Ag}^{+}$  are soft acid, and  $\text{Cu}^{2+}$ ,  $\text{Zn}^{2+}$ ,  $\text{Co}^{2+}$ ,  $\text{Mg}^{2+}$ ,  $\text{Ni}^{2+}$   
10  
11 200 and  $\text{Pb}^{2+}$  are borderline acid. Accordingly,  $\text{Cd}^{2+}$ ,  $\text{Cu}^{2+}$ ,  $\text{Ag}^{+}$ ,  $\text{Zn}^{2+}$ ,  $\text{Co}^{2+}$ ,  $\text{Mg}^{2+}$ ,  $\text{Ni}^{2+}$  and  
12  
13  
14 201  $\text{Pb}^{2+}$  could not conjugate with AD-MAH-RhB to form stable complexes, which were  
15  
16 202 the same as the experimental results. However, AD-MAH-RhB exhibited a specific  
17  
18  
19 203 selectivity to  $\text{Hg}^{2+}$  as well as  $\text{Fe}^{3+}$ , although  $\text{Hg}^{2+}$  is just a soft acid.

### 204 **3.2 Mechanism studies on the interaction between AD-MAH-RhB and metal ions**

205 In order to know the reason why AD-MAH-RhB could detect  $\text{Fe}^{3+}$  and  $\text{Hg}^{2+}$ , the  
206 interactions between AD-MAH-RhB and metal ions were investigated. In RhB-metal  
207 ion complexes, vibrational spectroscopy can provide information on coordination  
208 bond of metal ions and probes<sup>[30]</sup>. Thus, FTIR spectra of solid AD-MAH-RhB,  
209 AD-MAH-RhB@ $\text{Zn}^{2+}$ , AD-MAH-RhB@ $\text{Fe}^{3+}$  and AD-MAH-RhB@ $\text{Hg}^{2+}$  were  
210 recorded, and the resultant spectra are shown in Figure 3. Peaks at 3076 and 1676  
211  $\text{cm}^{-1}$  assigned to the cis-acylamino and amide groups (Figure 3a), respectively. After  
212 adding  $\text{Fe}^{3+}$ , the peak at 3076  $\text{cm}^{-1}$  disappeared and the peak at 1676  $\text{cm}^{-1}$  shifted to  
213 1670  $\text{cm}^{-1}$  (Figure 3c), indicating that  $\text{Fe}^{3+}$  influenced the acylamino and amide  
214 groups. After AD-MAH-RhB conjugated with  $\text{Hg}^{2+}$ , peaks at 3076 and 1676  $\text{cm}^{-1}$   
215 chemical shifted to 3056 and 1674  $\text{cm}^{-1}$ , and the peaks decreased slightly (Figure 3d).  
216 However, there was almost no change when adding  $\text{Zn}^{2+}$  and other metal ions (Figure  
217 3b, AD-MAH-RhB@ $\text{Zn}^{2+}$  as an example). These results suggested that  $\text{Fe}^{3+}$  and  $\text{Hg}^{2+}$   
218 (especially  $\text{Fe}^{3+}$ ) bound with acylamino and amide groups in AD-MAH-RhB, whereas

other metal ions have no reaction with AD-MAH-RhB. Moreover, peak at  $1632\text{ cm}^{-1}$  assigned to double carbon groups. After adding  $\text{Hg}^{2+}$  (Figure 3d), the absorbance at  $1632\text{ cm}^{-1}$  decreased, and a new peak at  $1530\text{ cm}^{-1}$  appeared, which belonged to cyclic olefin, suggesting that Hg acted as a bridge to cooperate with the two double bonds to form the cyclic olefin. These results indicated that  $\text{Fe}^{3+}$  mainly bound to amide and carbonyl groups to form AD-MAH-RhB@ $\text{Fe}^{3+}$  complex, while  $\text{Hg}^{2+}$  conjugated with amide, carbonyl and double carbon groups to form the AD-MAH-RhB@ $\text{Hg}^{2+}$  complex.

Since mass of probe changed after conjugated with metal ions<sup>[31]</sup>, mass spectroscopy was carried out to investigate the selectivity of AD-MAH-RhB to  $\text{Fe}^{3+}$  and  $\text{Hg}^{2+}$ . The theoretical mass of AD-MAH-RhB@ $\text{Hg}^{2+}$  is about 916. However, the related peak was not captured. On the contrary, peak at  $m/z \sim 815$  assigned to [AD-MAH-RhB@ $\text{Hg}^{2+}$ @AD-MAH-RhB]/2 (Figure 4a) was clearly observed in the mass spectrum of the AD-MAH-RhB@ $\text{Hg}^{2+}$  complex, indicating formation of 1:2 stoichiometry complex of  $\text{Hg}^{2+}$  and AD-MAH-RhB, as shown in Scheme 2a. In the case of AD-MAH-RhB@ $\text{Fe}^{3+}$ , a peak at  $m/z$  851.4 emerged in the MS spectrum for the AD-MAH-RhB@ $\text{Fe}^{3+}$  complex (Figure 4b). This result suggested the formation of [ $\text{Fe}^{3+}$ @AD-MAH-RhB@ $\text{Fe}^{3+}$ ] complex, i.e. formation of a 2:1 stoichiometry complex of  $\text{Fe}^{3+}$  and AD-MAH-RhB. Based on the results of FTIR spectra and mass analysis, the possible sensing mechanisms of AD-MAH-RhB complex with  $\text{Hg}^{2+}$  and  $\text{Fe}^{3+}$  are proposed in Scheme 2.

For further understand the selectivity of AD-MAH-RhB to  $\text{Fe}^{3+}$ , but not to  $\text{Ba}^{2+}$  and

241  $K^+$ , computational simulations were performed with GAUSSIAN03<sup>[26]</sup>. Ab initio DFT  
 242 using the well-established Becke three-parameter hybrid functional<sup>[32]</sup> with the  
 243 correlation functional of Lee, Yang and Parr<sup>[33]</sup> (B3LYP) was used, combined with  
 244 6-31G\* basis set, of which the abilities to calculate the structure and energy of the  
 245 probe have been widely demonstrated. The optimized structure was checked to be a  
 246 true minimum and not a saddle point by calculation, as shown in Figure 5a. From the  
 247 result of the ab initio calculation, the bond lengths of C-N, N-N and O-N are 2.34, 3.0  
 248 and 2.86 Å, respectively. Then, the spaces of the probe constituted by amine and  
 249 oxygen atom could be calculated to 3.28 Å. Therefore, Fe ion ( $d_{Fe}=2.52$  Å, d means  
 250 diameter) was perfectly suitable for the spaces, whereas the same hard acid such as  
 251  $Ba^{2+}$  ( $d_{Ba}=4.3$  Å) and  $K^+$  ( $d_K=4.4$  Å) were too big to suit the spaces.

252 On the other hand, when a probe and metal ion forms a stable complex, the bond  
 253 distance of Van der Waals between recognition groups and metal ion should be less  
 254 than the sum of Van der Waals radius of elements<sup>[34]</sup>. Otherwise, it is considered that  
 255 there is no interaction between the probe and metal ion. In the optimized structure of  
 256 AD-MAH-RhB@Fe<sup>3+</sup> complex by computational simulations (Figure 5b), the  
 257 distances of Fe-O and Fe-N are 1.9 and 1.95 Å, which are less than the sum of Van  
 258 der Waals radius of N (1.5 Å), O (1.5 Å) and Fe (2.23 Å)<sup>[35,36]</sup>. Therefore, Fe<sup>3+</sup> could  
 259 conjugate with AD-MAH-RhB probe to form stable complex, which induced by  
 260 synergetic effects of the suitable space and distance of Van der Waals.

### 261 3.3 Improving sensitivity and selectivity of PMAH-CD/AD-MAH-RhB

262 In order to improve the selectivity of the AD-MAH-RhB probe towards Fe ions, the

interaction between  $\text{Hg}^{2+}$  and AD-MAH-RhB should be prevented. Increasing inter- and intra- molecular interactions of AD-MAH-RhB might be a good way to reduce the reaction chance between AD-MAH-RhB and  $\text{Hg}^{2+}$ . Therefore, PMAH-CD was employed to prepare a supramolecular complex with AD-MAH-RhB by host-guest interaction. The inclusive complex formation was confirmed by  $^1\text{H}$ NMR spectrum, as shown in Figure S3. Fluorescence and UV-vis spectra confirmed that the colorless PMAH-CD/AD-MAH-RhB solution did not exhibit any absorption, which was coincident with the property of the spirocycle RhB derivatives. Addition of  $\text{Fe}^{3+}$  into the PMAH-CD/AD-MAH-RhB solution induced a significant color change to rose pink (inset photo in Figure 6a). Meanwhile, obvious changes in the absorption spectra at 564 nm appeared with addition of  $\text{Fe}^{3+}$ , which was similar to Figure 1a, due to the formation of the open-ring state of the RhB moieties. While, there was negligible absorbance of PMAH-CD/AD-MAH-RhB in the present of  $\text{Hg}^{2+}$  and other metal ions such as  $\text{Cd}^{2+}$ ,  $\text{Cu}^{2+}$ ,  $\text{Ba}^{2+}$ ,  $\text{Ag}^+$ ,  $\text{Zn}^{2+}$ ,  $\text{Co}^{2+}$ ,  $\text{K}^+$ ,  $\text{Mg}^{2+}$ ,  $\text{Ni}^{2+}$  (Figure 6a). Moreover, a dramatic change at 587 nm in the fluorescence spectrum was also observed upon addition of  $\text{Fe}^{3+}$ , while no obvious fluorescence appeared with addition of other metal ions, even  $\text{Hg}^{2+}$ , as shown in Figure 6b. These results confirmed that PMAH-CD/AD-MAH-RhB could detect  $\text{Fe}^{3+}$  to form binding complex, whereas not conjugate with  $\text{Hg}^{2+}$ .

The selectivity of PMAH-CD/AD-MAH-RhB towards  $\text{Fe}^{3+}$  over other metal ions was also investigated by the competitive experiments. Figure 7 shows the fluorescence intensity of PMAH-CD@AD-MAH-RhB in the present of  $\text{Fe}^{3+}$  only and

285  $\text{Fe}^{3+}$  mixed with 100 equiv of various metal ions at 587 nm of emission peak. The  
 286 results showed that the  $\text{Fe}^{3+}$  induced fluorescence enhancement was not obviously  
 287 affected in the presence of other ions. The selectivity and competition experiments  
 288 revealed that PMAH-CD@AD-MAH-RhB has a remarkable selectivity towards  $\text{Fe}^{3+}$ .

### 289 **3.4 Mechanism studies on the interaction between PMAH-CD/AD-MAH-RhB** 290 **and metal ions**

291 When AD-MAH-RhB is as a guest to form the complex with PMAH-CD,  
 292 PMAH-CD/AD-MAH-RhB can dissolve in ultrapure water and from lots of  
 293 interactions of intramolecular and intermolecular hydrogen bonds, inducing the chains  
 294 entangled and network formation. Since one  $\text{Hg}^{2+}$  needed two AD-MAH-RhB  
 295 molecules to form a complex, as mentioned above, the high hydrogen interactions of  
 296 among PMAH-CD/AD-MAH-RhB probes might prevent AD-MAH-RhB from  
 297 closing each other and also prevent  $\text{Hg}^{2+}$  from conjugating with two  
 298 PMAH-CD/AD-MAH-RhB. However,  $\text{Fe}^{3+}$  ions just need one molecule  
 299 AD-MAH-RhB, and these hydrogen bonds had no effect on the reactive space and  
 300 distance of Van der Waals. This is why PMAH-CD@AD-MAH-RhB has a good  
 301 selectivity for  $\text{Fe}^{3+}$  in the presence of  $\text{Hg}^{2+}$ . Unfortunately, the interactions between  
 302 PMAH-CD/AD-MAH-RhB probes and between PMAH-CD/AD-MAH-RhB and  
 303 metal ions are difficult to calculate by computational simulations, because of  
 304 complicated structure of the supermolecular structure. Anyway, the modified probe  
 305 showed the high selectivity towards  $\text{Fe}^{3+}$ .

### 306 **4 Conclusion**



1  
2  
3  
4 307 A novel probe composed of rhodamine derivative AD-MAH-RhB was synthesized,  
5  
6 308 and it showed sensitivity to  $\text{Fe}^{3+}$ . However,  $\text{Hg}^{2+}$  was found to disturb the detection.  
7  
8  
9 309 The mechanism and interaction between the probe and metal ions were studied based  
10  
11 310 on computational simulations, HSAB principle, and FTIR and mass spectra. The  
12  
13 311 results suggested that  $\text{Fe}^{3+}$  was suitable to the probe structure and the bond distance of  
14  
15  
16 312 Van der Waals was less than the sum of Van der Waals radius of elements. Moreover,  
17  
18  
19 313  $\text{Fe}^{3+}$  bound with amine and oxygen atoms in AD-MAH-RhB to form a complex  
20  
21 314 composed of 2:1 stoichiometry of  $\text{Fe}^{3+}$  and AD-MAH-RhB, whereas  $\text{Hg}^{2+}$  bound with  
22  
23 315 amine, oxygen atoms and double carbon groups in AD-MAH-RhB to form a complex  
24  
25  
26 316 composed of 1:2 stoichiometry of  $\text{Hg}^{2+}$  and AD-MAH-RhB. For improvement of the  
27  
28  
29 317 selectivity of the probe, PMAH-CD was employed to inclusive AD-MAH-RhB to  
30  
31 318 form another probe. PMAH-CD/AD-MAH-RhB showed excellent selectivity and  
32  
33  
34 319 sensitivity towards the detection of  $\text{Fe}^{3+}$  in aqueous solution. The high hydrogen  
35  
36  
37 320 interactions existing among the probes might inhibit the form stable complex with  
38  
39 321  $\text{Hg}^{2+}$ . The novel probes could be used as the fluorescence sensors to detect metal ions  
40  
41  
42 322 in aqueous solution. The mechanism studies might help to design and construct novel  
43  
44 323 fluorescence sensors effectively and well understand the interaction between the  
45  
46  
47 324 probe and metal ions.

#### 48 49 325 **Acknowledgements**

50  
51 326 This study was supported by the National Natural Science Foundation of China (No.  
52  
53 327 21004029 and 51173072), MOE & SAFEA for the 111 Project (B13025), the  
54  
55  
56 328 Fundamental Research Funds for the Central Universities (JUSRP51408B) and the  
57  
58  
59  
60

329 Enterprise-university-research prospective program, Jiangsu Province (No.  
330 BY2012057).

331 **References**

- 332 1. L. Prodi, C. Bargossi, M. Montalti, N. Zaccheroni, N. Su, J. S. Bradshaw, R. M.  
333 Izatt and P. B. Savage, An Effective Fluorescent Chemosensor for Mercury Ions. J.  
334 Am. Chem. Soc., 2000, 122, 6769-6770.
- 335 2. Xiaohua Li, Xinghui Gao, Wen Shi, Huimin Ma, Design Strategies for  
336 Water-Soluble Small Molecular Chromogenic and Fluorogenic Probes, Chem.  
337 Rev., 2014, 114 (1), 590–659
- 338 3. H. N. Kim, W. X. Ren, J. S. Kim and J. Yoon, Fluorescent and colorimetric  
339 sensors for detection of lead, cadmium, and mercury ions. Chem. Soc. Rev., 2012,  
340 41, 3210-3244.
- 341 4. G. K. Darbha, A. Ray and P. C. Ray, Gold Nanoparticle-Based Miniaturized  
342 Nanomaterial Surface Energy Transfer Probe for Rapid and Ultrasensitive  
343 Detection of Mercury in Soil, Water, and Fish. ACS nano, 2007, 1, 208-214.
- 344 5. X. F. Guo, X. H. Qian and L. H. Jia, A Highly Selective and Sensitive Fluorescent  
345 Chemosensor for Hg<sup>2+</sup> in Neutral Buffer Aqueous Solution. J. Am. Chem. Soc.,  
346 2004, 126, 2272-2273.
- 347 6. Y. N. Li, H. Huang, Y. Li, X. G. Su, Highly sensitive fluorescent sensor for  
348 mercury (II) ion based on layer-by-layer self-assembled films fabricated with  
349 water-soluble fluorescent conjugated polymer. Sensor Actuat. B, 2013, 188,  
350 772-777.

- 1  
2  
3  
4 351 7. J. F. Li , Y. Z. Wu, F. Y. Song, G. Wei, Y. X. Cheng and C. J. Zhu, A highly  
5  
6 352 selective and sensitive polymer-based OFF-ON fluorescent sensor for Hg<sup>2+</sup>  
7  
8 353 detection incorporating salen and perylenyl moieties. J. Mater. Chem., 2012, 22,  
9  
10 354 478-482.
- 11  
12  
13 355 8. J. M. Hu, T. Wu, G. Q. Zhang and S. Y. Liu, Highly Selective Fluorescence  
14  
15 356 Sensing of Mercury Ions over a Broad Concentration Range Based on Mixed  
16  
17 357 Polymeric Micelles. Macromolecules, 2012, 45, 3939-3947.
- 18  
19 358 9. X. J. Wan, S. Yao, H. Y. Liu and Y. W. Yao, Selective fluorescence sensing of  
20  
21 359 Hg<sup>2+</sup> and Zn<sup>2+</sup> ions through dual independent channels based on the site-specific  
22  
23 360 functionalization of mesoporous silica nanoparticles. J. Mater. Chem. A , 2013, 1,  
24  
25 361 10505-10512.
- 26  
27 362 10. J. Du, M. Y. Liu, X. H. Lou, T. Zhao, Z. Wang, Y. Xue, J. L. Zhao and Y. S. Xu,  
28  
29 363 Highly Sensitive and Selective Chip-Based Fluorescent Sensor for Mercuric Ion:  
30  
31 364 Development and Comparison of Turn-On and Turn-Off Systems. Anal. Chem.,  
32  
33 365 2012, 84, 8060-8066.
- 34  
35 366 11. L. B. Zhang, T. Li, B. L. Li , J. Li and E. K. Wang, Carbon nanotube-DNA hybrid  
36  
37 367 fluorescent sensor for sensitive and selective detection of mercury(II) ion. Chem.  
38  
39 368 Commun., 2010, 46, 1476-1478.
- 40  
41 369 12. M. Taki, K. Akaoka, S. Iyoshi and Y. Yamamoto, Rosamine-Based Fluorescent  
42  
43 370 Sensor with Femtomolar Affinity for the Reversible Detection of a Mercury Ion.  
44  
45 371 Inorg. Chem., 2012, 51, 13075-13077.
- 46  
47 372 13. I. Kim, D. Kim, S. Sambasivan and K. H. Ahn, Synthesis of  $\pi$ -extended coumarins  
48  
49  
50  
51  
52  
53  
54  
55  
56  
57  
58  
59  
60

- and evaluation of their precursors as reactive fluorescent probes for mercury ions.
- Asian J. Org. Chem., 2012, 1, 60-64.
14. Q. Y. Chen and C. F. Chen, A new Hg<sup>2+</sup>-selective fluorescent sensor based on a dansyl amide-armed calix[4]-aza-crown. Tetrahedron Lett., 2005, 46, 165-168.
15. H. L. Mu, R. Gong and Q. Ma, A novel colorimetric and fluorescent chemosensor: synthesis and selective detection for Cu<sup>2+</sup> and Hg<sup>2+</sup>. Tetrahedron Lett., 2007, 48, 5525-5529.
16. X. B. Zhang, Z. Z. Li and G. L. Shen, An Optical Fiber Chemical Sensor for Mercury Ions Based on a Porphyrin Dimer. Anal. Chem., 2002, 74, 821-825.
17. J. K. Ni, Q. Y. Li, B. Li and L. M. Zhang, A novel fluorescent probe based on rhodamine B derivative for highly selective and sensitive detection of mercury(II) ion in aqueous solution. Sensor Actuat. B, 2013, 186, 278-285.
18. C. Wu, Q. N. Bian, B. G. Zhang, X. Cai, S. D. Zhang, H. Zheng, S. Y. Yang, Y. B. Jiang, Ring expansion of spiro-thiolactam in rhodamine scaffold: switching the recognition preference by adding one atom. Org. Lett., 2012, 14, 4198-4201.
19. Zhiguo Zhou, Mengxiao Yu, Hong Yang, Kewei Huang, Fuyou Li, Tao Yi, Chunhui Huang, FRET-based sensor for imaging chromium(III) in living cells [J] Chem. Comm., 2008, (29):3387-3389.
20. Zhi-Qiang Hu, Xiao-Ming Wang, Yong-Cheng Feng, Lei Ding, Ming Li, Cun-Sheng Lin, A novel colorimetric and fluorescent chemosensor for acetate ions in aqueous media based on a rhodamine 6G-phenylurea conjugate in the presence of Fe(III) ions, Chem. Comm., 2011, 47(5):1622 — 1624.

- 1  
2  
3  
4 395 21. Young-Keun Yang, Keun-Jeong Yook, Jinsung Tae, A Rhodamine-Based  
5  
6 396 Fluorescent and Colorimetric Chemodosimeter for the Rapid Detection of Hg<sup>2+</sup>  
7  
8 397 Ions in Aqueous Media. *J. Am. Chem. Soc.*, 2005, 127 (48), 16760–16761.  
9  
10  
11 398 22. Hyemi Kim, Sunho Lee, Jihyun Lee, Jinsung Tae, Rhodamine Triazole-Based  
12  
13 399 Fluorescent Probe for the Detection of Pt, *Org. Lett.*, 2010, 12 (22), 5342–5345  
14  
15  
16 400 23. Xiao Tian, Xiangping Zhang, Lu Wei, Shaojuan Zeng, Lei Huang, Suojian Zhang,  
17  
18 401 Multi-scale simulation of the 1,3-butadiene extraction separation process with an  
19  
20 402 ionic liquid additive, *Green Chem.*, 2010, 12, 1263–1273.  
21  
22  
23 403 24. Pearson B G. Hard and Soft Acids and Bases. *J Am Chem Soc.* 1963,85,3533.  
24  
25  
26 404 25. J. Luo, S. S. Jiang, S. H. Qin, H. Q. Wu, Y. Wang, J. Q. Jiang and X. Y. Liu,  
27  
28 405 Highly sensitive and selective turn-on fluorescent chemosensor for Hg<sup>2+</sup> in pure  
29  
30 406 water based on a rhodamine containing water-soluble copolymer. *Sensors and*  
31  
32 407 *Actuators B*, 2011, 160, 1191-1197.  
33  
34  
35 408 26. M. J. Frisch, G. W. Trucks, H. B. Schlegel, G. E. Scuseria, M. A. Robb, J. R.  
36  
37 409 Cheeseman, J. A. Montgomery, Jr., T. Vreven, K. N. Kudin, J. C. Burant,  
38  
39 410 J.M. Millam, S. S. Iyengar, J. Tomasi, V. Barone, B. Mennucci, M. Cossi, G.  
40  
41 411 Scalmani, N. Rega, G. A. Petersson, H. Nakatsuji, M. Hada, M. Ehara, K. Toyota, R.  
42  
43 412 Fukuda, J. Hasegawa, M. Ishida, T. Nakajima, Y. Honda, O. Kitao, H. Nakai, M.  
44  
45 413 Klene, X. Li, J. E. Knox, H. P. Hratchian, J. B. Cross, V. Bakken, C. Adamo, J.  
46  
47 414 Jaramillo, R. Gomperts, R. E. Stratmann, O. Yazyev, A. J. Austin, R. Cammi, C.  
48  
49 415 Pomelli, J. Ochterski, P. Y. Ayala, K. Morokuma, G. A. Voth, P. Salvador, J. J.  
50  
51 416 Dannenberg, V. G. Zakrzewski, S. Dapprich, A. D. Daniels, M. C. Strain, O.  
52  
53  
54  
55  
56  
57  
58  
59  
60

- 417 Farkas, D. K. Malick, A. D. Rabuck, K. Raghavachari, J. B. Foresman, J. V. Ortiz,  
418 Q. Cui, A. G. Baboul, S. Clifford, J. Cioslowski, B. B. Stefanov, G. Liu, A.  
419 Liashenko, P. Piskorz, I. Komaromi, R. L. Martin, D. J. Fox, T. Keith, M. A.  
420 Al-Laham, C. Y. Peng, A. Nanayakkara, M. Challacombe, P. M. W. Gill, B. G.  
421 Johnson, W. Chen, M. W. Wong, C. Gonzalez and J. A. Pople, GAUSSIAN 03  
422 (Revision C.02), Gaussian, Inc., Wallingford, CT, 2004.
- 423 27. John T. Lai, Debby Filla, Ronald Shea, Functional Polymers from Novel  
424 Carboxyl-Terminated Trithiocarbonates as Highly Efficient RAFT Agents.  
425 *Macromolecules*, 2002, 35, 6754-6756.
- 426 28. Y. Y. Liu, X. D. Fan, L. Gao, Synthesis and characterization of  $\beta$ -cyclodextrin  
427 based functional monomers and its copolymers with N-isopropylacrylamide.  
428 *Macromol. Biosci*, 2003, 3, 715–719.
- 429 29. Kong, Rui; Shi, Dongjian, Liu, Rongjin, Wu, Chao, Ni, Peihong, Chen, Mingqing,  
430 Preparation and Properties of Supramolecular Aggregation of Dual-Sensitive  
431 Cyclodextrins, *Acta Chim. Sinica* 2013, 71, 1540—1546
- 432 30. Ma LJ, Li Y, Li L, Wu YQ, Buchet R, Ding YH (2009) Larification of the Binding  
433 Model of Lead(II) with a Highly Sensitive and Selective Fluoroionophore Sensor  
434 by Spectroscopic and Structural Study, *Spectrochim. Acta A* 72: 306-311.
- 435 31. Qin W, Zou B, Zhang Y, Yi XH, Pan ZH (2013) UV-VIS, fluorescence and mass  
436 spectrometry investigation on the transition metal ion chelation of two bioisosteres  
437 of resveratrol, *Asian J Chem* 25: 2185-2188.
- 438 32. A. D. Becke, Density-functional thermochemistry. III. The role of exact exchange.

- 1  
2  
3  
4 439 J. Chem. Phys., 1993, 98, 5648–5652.  
5  
6 440 33. C. T. Lee, W. T. Yang and R. G. Parr, Development of the Colle-Salvetti  
7  
8 441 correlation-energy formula into a functional of the electron density. Phys. Rev. B:  
9  
10 442 Condens. Matter, 1988, 37, 785–789.  
11  
12  
13 443 34. Hu Shengzhi, Zhou Zhaohui, Tsai Khirui, Average Van der Waals radii actions in  
14  
15 444 crystals, Acta. Phys. Chim. Sin., 2003, 19, 1073-1077.  
16  
17  
18 445 35. Pauling L., The nature of the chemical bond. NY; Cornell Univ. Press, 1939.  
19  
20  
21 446 36. Allinger N.L., Zhou X., Bergsma J., Molecular mechanics parameters, J. Mol.  
22  
23 447 Struct., Theochem., 1994, 118, 69-83.  
24  
25  
26 448  
27  
28  
29  
30  
31  
32  
33  
34  
35  
36  
37  
38  
39  
40  
41  
42  
43  
44  
45  
46  
47  
48  
49  
50  
51  
52  
53  
54  
55  
56  
57  
58  
59  
60

**Figure Captions**

**Scheme 1.** Schematic representative of structures of AD-MAH-RhB (a) and PMAH-CD/AD-MAH-RhB (b).

**Figure 1.** (a) Absorption spectra and (b) Fluorescence spectra of AD-MAH-RhB aqueous solution at pH 7.0 with increasing concentration of  $\text{Fe}^{3+}$  from 0 to  $38 \text{ mg L}^{-1}$ . Inset photo shows the color change of AD-MAH-RhB solution upon the addition of  $\text{Fe}^{3+}$ .

**Figure 2.** Fluorescence intensity of the AD-MAH-RhB aqueous solution ( $1.4 \times 10^{-4} \text{ M}$ ) at 587 nm upon addition of different metal ions with the concentration of  $1 \times 10^{-2} \text{ M}$  in pH=7.0 by excitation at 541 nm. Inset photos show the colors of AD-MAH-RhB upon addition of different metal ions with the concentration of  $1 \times 10^{-2} \text{ M}$ .

**Figure 3.** FTIR spectra of AD-MAH-RhB (a), AD-MAH-RhB/ $\text{Zn}^{2+}$  (b), AD-MAH-RhB/ $\text{Fe}^{3+}$  (c), and AD-MAH-RhB/ $\text{Hg}^{2+}$  (d).

**Figure 4.** MS spectra of AD-MAH-RhB/ $\text{Hg}^{2+}$  (a) and AD-MAH-RhB/ $\text{Fe}^{3+}$  (b).

**Figure 5.** Visualization of the DFT-optimized (calculated at the B3LYP 6-31G\* level) structure of AD-MAH-RhB, nitrogen atoms are shown in blue, oxygen atoms in red, carbon atoms in dark gray, hydrogen atoms in white, and Fe ions in red brown.

**Scheme 2.** Proposed mechanisms for interactions of AD-MAH-RhB with  $\text{Hg}^{2+}$  (a) and  $\text{Fe}^{3+}$  (b).

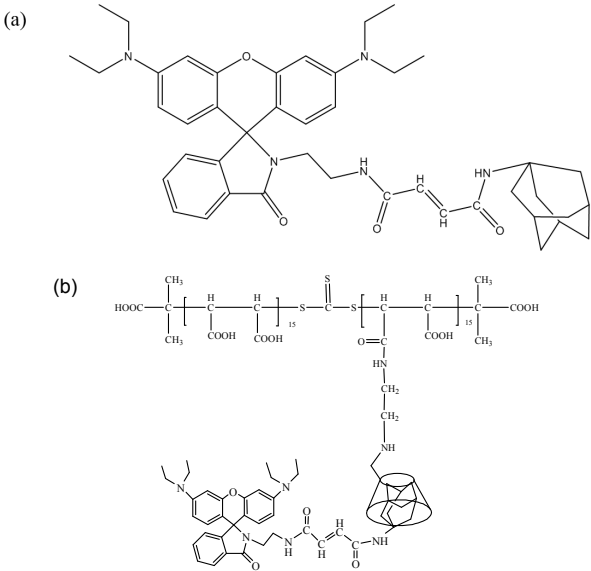
**Figure 6.** (a) Absorption and (b) Fluorescence intensity of the PMAH-CD/AD-MAH-RhB aqueous solution ( $1.4 \times 10^{-4} \text{ M}$ ) at 587 nm upon addition of different metal ions with the concentration of  $1 \times 10^{-2} \text{ M}$  in pH=7.0 by excitation at 541



471 nm. Inset photos show the colors of PMAH-CD/AD-MAH-RhB upon addition of  
472 different metal ions with the concentration of  $1 \times 10^{-2}$  M.

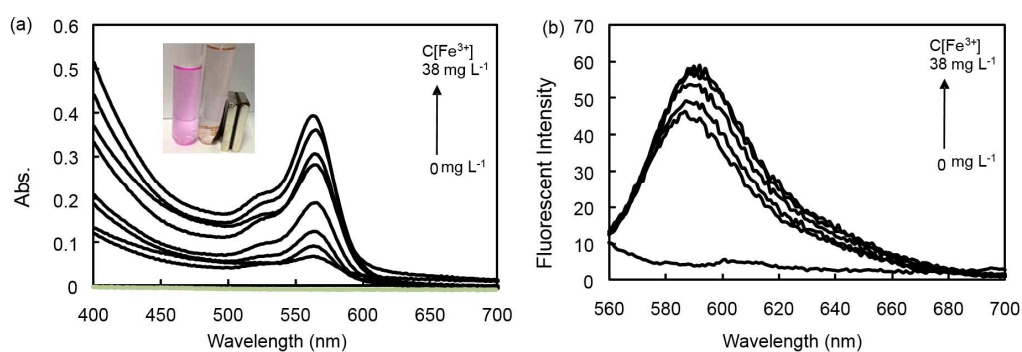
473 **Figure 7.** Fluorescence intensity of the PMAH-CD/AD-MAH-RhB aqueous solution  
474 ( $1 \times 10^{-4}$  M) upon addition of Fe ion ( $1 \times 10^{-4}$  M) in the presence of various metal ions  
475 ( $1 \times 10^{-2}$  M) in pH=7.0 at 541 nm of excitation wavelength.

476



Scheme 1. Shi et al.

482



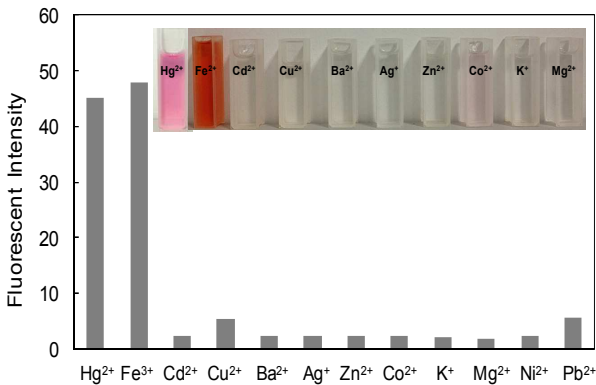
483

484

Figure 1. Shi et al.

485

486



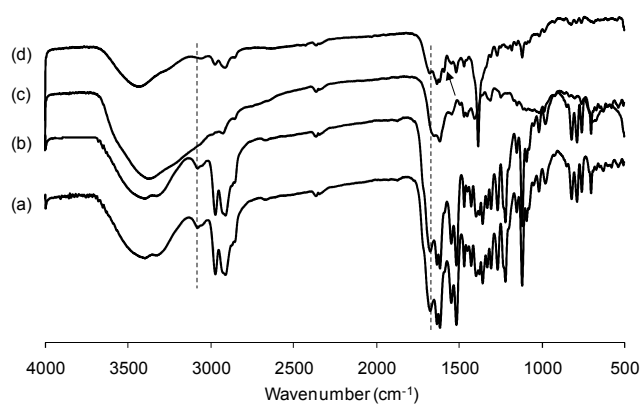
487

488

Figure 2. Shi et al.

489

490



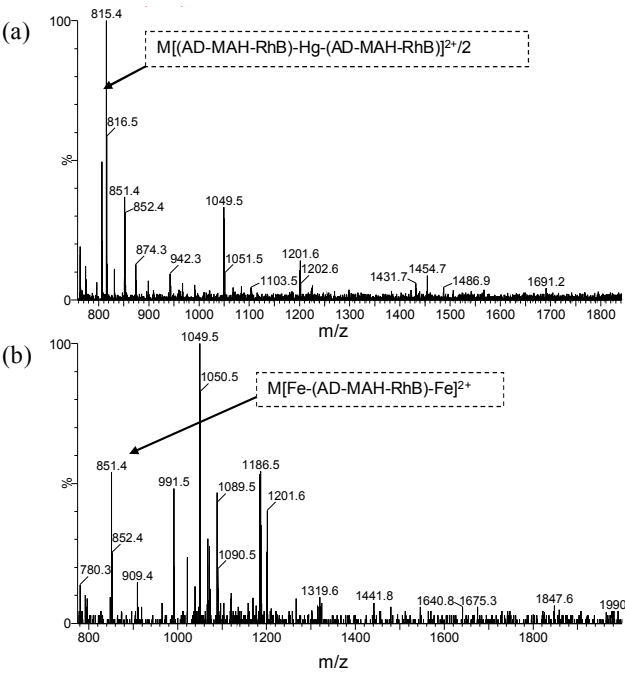
491

492

Figure 3. Shi et al.

493

494



495

496

497

Figure 4. Shi et al.

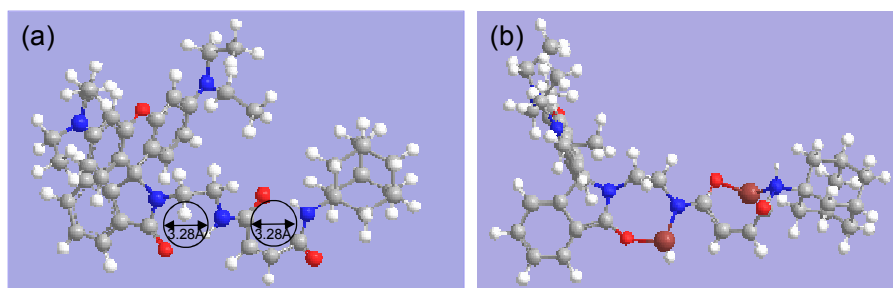
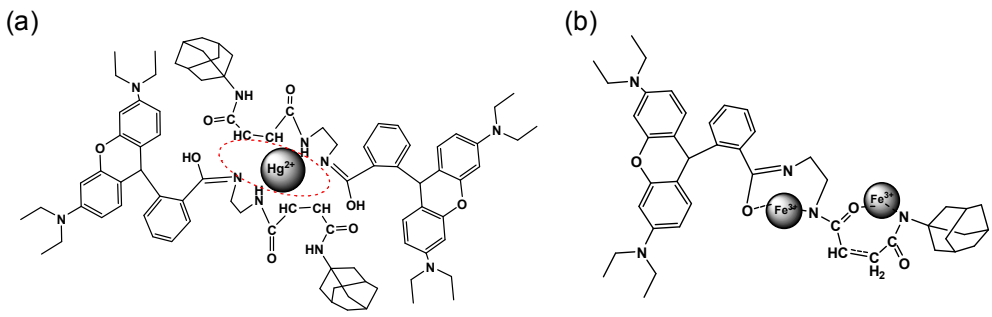


Figure 5. Shi et al.



Scheme 2. Shi et al.



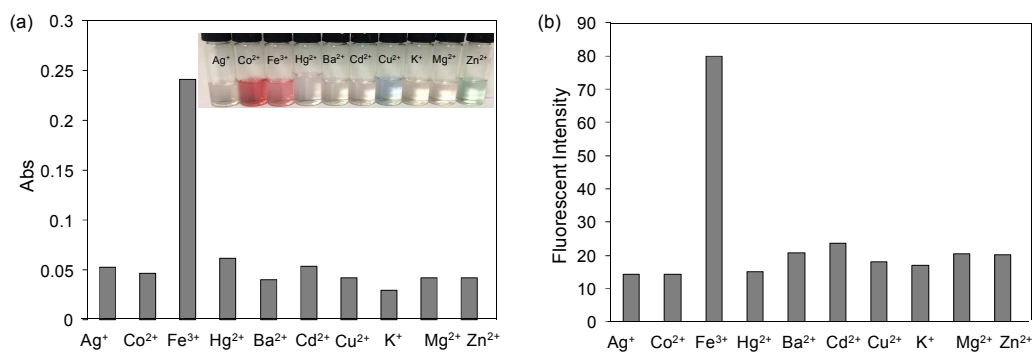
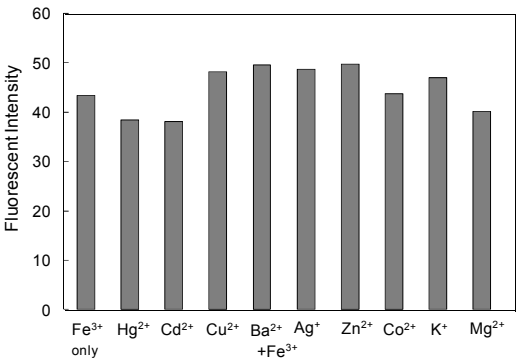


Figure 6. Shi et al.

511



512

513

Figure 7. Shi et al.

514

